Jeffrey A. McGuire
STRETCH Lab,
Department of Biomedical
Engineering and Mechanics,
Virginia Tech,
Blacksburg, VA 24061
e-mail: jeffmcg8@vt.edu

Steven D. Abramowitch
Department of Bioengineering,
University of Pittsburgh,
Pittsburgh, PA 15261
e-mail: sdast9@pitt.edu

Spandan Maiti
Department of Bioengineering,
University of Pittsburgh,
Pittsburgh, PA 15261
e-mail: spm54@pitt.edu

Raffaella De Vita
STRETCH Lab,
Department of Biomedical
Engineering and Mechanics,
Virginia Tech,
Blacksburg, VA 24061
e-mail: devita@vt.edu

Swine Vagina Under Planar Biaxial Loads: An Investigation of Large Deformations and Tears

Vaginal tears are very common and can lead to severe complications such as hemorrhaging, fecal incontinence, urinary incontinence, and dyspareunia. Despite the implications of vaginal tears on women's health, there are currently no experimental studies on the tear behavior of vaginal tissue. In this study, planar equi-biaxial tests on square specimens of vaginal tissue, with sides oriented along the longitudinal direction (LD) and circumferential direction (CD), were conducted using swine as animal model. Three groups of specimens were mechanically tested: the NT group ($n = 9$), which had no pre-imposed tear, the longitudinal tear (LT) group ($n = 9$), and the circumferential tear (CT) group ($n = 9$), which had central pre-imposed elliptically shaped tears with major axes oriented in the LD and the CD, respectively. Through video recording during testing, axial strains were measured for the NT group using the digital image correlation (DIC) technique and axial displacements of hook clamps were measured for the NT, LT, and CT groups in the LD and CD. The swine vaginal tissue was found to be highly nonlinear and somewhat anisotropic. Up to normalized axial hook displacements of 1.15, no tears were observed to propagate, suggesting that the vagina has a high resistance to further tearing once a tear has occurred. However, in response to biaxial loading, the size of the tears for the CT group increased significantly more than the size of the tears for the LT group ($p = 0.003$). The microstructural organization of the vagina is likely the culprit for its tear resistance and orientation-dependent tear behavior. Further knowledge on the structure–function relationship of the vagina is needed to guide the development of new methods for preventing the severe complications of tearing. [DOI: 10.1115/1.4042437]

1 Introduction

Vaginal tears are wounds that occur in or around the vagina and may drastically vary in severity from superficial cuts of the mucosal lining to tears propagating through the entire vaginal wall and into the surrounding muscle and organs. These tears may result from intercourse, traumatic injuries, or large hormonal changes through aging and menopause [1–3]. However, the most common cause of vaginal tearing is childbirth. The vagina must expand from a diameter of ~2.5 cm to a diameter of ~9.5 cm to allow the passage of a full term baby [4,5]. Up to 90% of women experience tearing during vaginal delivery [6,7], and the reported number of severe tears is increasing as the number of cesarean deliveries decreases and as physicians and hospitals are improving awareness and protocols for examining and reporting tears [8–10]. Because the vagina is highly vascular in nature and represents the central support structure of the pelvic floor, tearing can result in complications including traumatic postpartum hemorrhaging [11], fecal or urinary incontinence [12,13], or dyspareunia [14]. These conditions can persist for many years producing emotional and psychological trauma in addition to physical pain [15,16].

Risk factors for tears during labor (e.g., episiotomies, birth weight, birthing position, and duration of the delivery), as well as possible techniques for mitigating these tears, have been investigated extensively [17]. However, the observed correlations between risk factors, tear occurrence, and management methods remain empirical. The behavior of a tear is strongly dependent on the microstructural and mechanical properties of the vagina and surrounding pelvic floor tissues. Knowledge of these properties will help determine the reasons for the observed correlations, and they will allow prediction of the occurrence and severity of tears, the impact on the patients' health, and the outcomes of prevention and treatment methods.

The vagina is a fibromuscular multilayered organ that is comprised of four layers: the epithelium, the lamina propria, the muscularis, and the adventitia [18]. Several studies have been published on the structure and composition of the vaginal tissue [19–23] but, due to the differences in animal models, tissue collection protocols, and experimental methods, the available histological results are difficult to compare and often contradictory [24,25]. Regardless, the vaginal wall has been found to be primarily made of collagen, smooth muscle, and elastin, with regional differences in composition along the length of the vagina [22,23]. Smooth muscle cells are organized into two indistinguishable layers and are oriented in the longitudinal direction (LD) and circumferential direction (CD), but data on the organization of collagen and elastin fibers remain limited [26].

Existing research has focused on characterizing the mechanical properties of the vagina but has failed to quantify the behavior of tears. The vast majority of the work in this area has been done via uniaxial tensile tests as reviewed in detail elsewhere [27], but some recent work has been carried out using more physiologically relevant biaxial tests [28]. In general, the vaginal tissue has been observed to exhibit a nonlinear anisotropic behavior with tissue being stiffer more often in the LD compared to the CD. While there are no mechanical studies that examine the tear behavior of vaginal tissue, tearing in other soft biological tissues has been investigated [29–34]. Uniaxial and biaxial tests have been performed on specimens with a pre-imposed notch or tear in order to analyze the tear propagation. During testing, as the specimens were subjected to tension, the fibers reoriented toward the direction of loading and localized at the tip of the defects providing local resistance to tearing [33,34]. The ability of fibers to reorient

Manuscript received June 8, 2018; final manuscript received December 3, 2018; published online February 13, 2019. Assoc. Editor: Thao (Vicky) Nguyen.

and reorganize is strongly linked to the mobility of water in soft tissues and may give rise to the strong defect tolerance of soft tissues [34].

This study aims to, for the first time, quantify the deformation and tear behavior of the vagina under planar biaxial loading. Histological analysis of the swine vaginal tissue is conducted to confirm similarities in the anatomy and morphology of the vaginal wall between swine and humans [35,36]. Using the digital image correlation (DIC) technique [37], we measure the local large strains experienced by the tissue along the two axial loading directions, the LD and CD. We also examine the effects of an elliptically shaped pre-imposed tear with major axes oriented along the LD or CD on the remote stresses and describe the size changes of the pre-imposed tear. The findings of this study on the deformations and tear behavior of the vagina have the potential to advance women's health by suggesting new analytically based approaches for preventing and treating tears.

2 Methods

2.1 Specimen Preparation. This study was conducted with the approval of the Institutional Animal Care and Use Committee (IACUC) at Virginia Tech. Reproductive tracts from eleven adult domestic swine (3–4 years old, ~450 lbs.) were obtained from a local slaughterhouse (Gunnoe Sausage Company, Goode, VA), and the vaginal canals were isolated between the interdigitating mucosal folds of the cervix (*pulvini cervicales*) and the introitus. Ten vaginal walls were used for mechanical testing and one was used for preliminary histological analysis. Vaginal wall tissue for mechanical testing was cut longitudinally along the urethra, hydrated with phosphate-buffered saline (PBS, *p*H 7.4, Fisher Scientific, Hampton, NH), and stored at −20 °C until testing. For histology, a total of 12 specimens were harvested and immediately placed in a 10% buffered formalin solution. Specifically, four specimens were obtained from the cranial region, four from the middle region, and four from the caudal region of the vagina. In each region, two specimens were oriented with the cross section in the LD and two with the cross section in the CD (Fig. 1).

2.2 Histology. Swine specimens were gradually dehydrated in a graded ethanol and xylol series, embedded in paraffin wax, and cut into 4 μm thin sections with a microtome. From each (cranial, middle, or caudal) region, two cross section specimens, one in the LD and the other in the CD, were stained with Masson's trichrome (MT) stain and two cross section specimens, one in the LD and the other in the CD, were stained with Verhoeff-van Gieson (VVG) stain (Fig. 1). The histological slides were examined under a light microscope (DMI6000B, Leica Microsystems, Bannockburn, IL) equipped with a scanning stage (LMT260, Leica Microsystems, Bannockburn, IL) at 10× magnification, and images were collected using a digital microscope camera (DMC4500, Leica Microsystems, Bannockburn, IL). Full specimen images were taken and then processed with an ImageJ plug-in (NIH, Bethesda, MD) to detect different colors. Smooth muscle and collagen contents were quantified from the MT-stained slides while elastin content was quantified from the VVG-stained slides. Briefly, blue for collagen and red for smooth muscle from the MT-stained slides as well as black for elastin from the VVG-stained slides were detected from each image, and the percent areas of each color over the areas of the full specimen images were calculated.

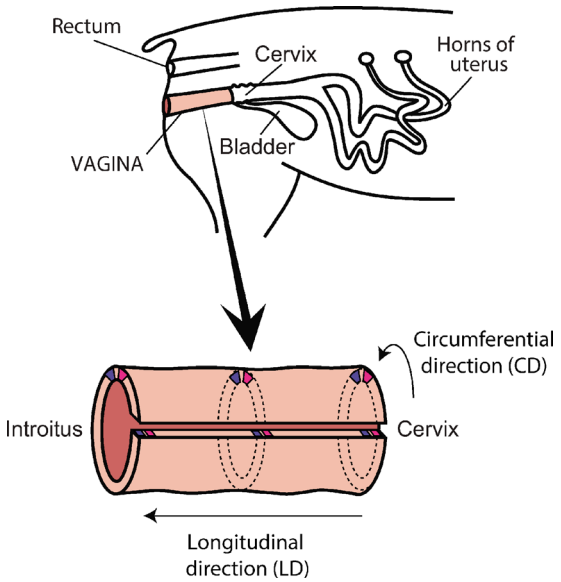

Fig. 1 Diagram of the vaginal tract within the swine displaying the three regions and two cross sections from which samples were taken for histological analysis. Blue squares represent specimens stained with MT stain and magenta squares represent specimens stained with VVG stain.

2.3 Testing Protocol. The vaginal tissue was thawed in PBS at room temperature (20–25 °C), cut into approximately $3.5 \times 3.5\,\text{cm}^2$ square specimens from the upper two-thirds of the vaginal wall with the two sides oriented along the LD and CD, and dyed blue with an aqueous methylene blue solution (1% w/v) for optical contrast. Three groups were tested in this study: a no tear (NT) group ($n = 9$), a longitudinal tear (LT) group ($n = 9$), and a circumferential tear (CT) group ($n = 9$) for a total of $n = 27$ specimens. Each specimen's thickness was measured with digital calipers (accuracy ±0.05 mm, Mitutoyo Absolute Low Force Calipers Series 573, Japan) under a 50 g compressive load and then clamped with four custom-made hooks. The average thickness of specimens in each group is reported in Table 1. For the specimens in the LT and CT groups, surgical scissors were used to cut an approximately central tear oriented with its major axis in the LD and CD, respectively. The average length of the tears for the two groups is also reported in Table 1. Specimens were speckled with an aerosol fast dry gloss white paint (McMaster-Carr, Elmhurst, IL) to create a speckle pattern for noncontact strain measurement methods [38]. Throughout the preparation process, the specimens were hydrated with PBS.

High-resolution (1600 × 1200 pixels) images of the specimens were taken during testing at one frame per second (fps) via two CCD cameras (Prosilica GX 1660, Allied Vision Technologies, Exton, PA) equipped with macro lenses (AT-X 100 mm F2.8 AT-X M100 Pro D Macro Lens, Tokina, Tokyo, Japan). Noncontact strain measurements were performed with a 3D-DIC system (Vic-3D 7, Correlated Solutions, Columbia, SC) by closely following the system testing guide and manual provided. The system was calibrated prior to every test by taking images of a $12 \times 9\,\text{mm}^2$ plastic grid with 4 mm spacing. All specimens were immersed within an acrylic glass bath (Perspex, UK) filled with PBS at room temperature (approximately 21 °C) and mounted onto an Instron planar biaxial machine with 50 N load cells

Table 1 Measurements of specimen thickness, distances between hooks, lengths of the major and minor axes of the tear, areas of the tear in the undeformed configuration as defined in Fig. 2. Data are reported as mean ± standard deviation.

	NT ($n = 9$)	LT ($n = 9$)	CT ($n = 9$)
Thickness, mm	3.32 ± 0.32	3.26 ± 0.72	2.95 ± 0.60
H_{LD}, mm	29.28 ± 3.95	28.06 ± 2.29	27.46 ± 2.19
H_{CD}, mm	29.14 ± 2.36	31.04 ± 2.96	33.47 ± 3.87
2A, mm	—	14.93 ± 1.44	16.73 ± 2.7
2B, mm	—	5.70 ± 1.83	5.37 ± 0.84
$\mathcal{A}$, mm^2	—	62.56 ± 18.92	69.06 ± 19.54

(accuracy ±0.05 N, Instron, High Wycombe, UK). The specimens were mounted with the epithelial layer exposed to the cameras. The bath was covered with an acrylic glass cover that created a flat planar surface with the PBS to ensure the fluid would not interfere with DIC measurements. Specimens were preconditioned by applying equibiaxial loads from 0.2 N to 1 N at a displacement rate of 0.1 mm/s for ten cycles. They were unloaded and allowed to recover for 600 s (= 10 min), and then equibiaxially preloaded to 0.2 N. They were then pulled at a displacement rate of 0.1 mm/s.

The collected data were analyzed until either the specimens were observed to tear at the hooks or the pre-imposed tears began to propagate. This assessment was qualitative and performed by reviewing the recorded image sequences of each test at every 15th frame (every 15 s). Due to the speckle patterns placed on the specimens, tears at the hooks were easily observed. Once the movement of the speckles in the vicinity of any hook was observed to abruptly change directions, the test was deemed compromised and data analysis was terminated. Moreover, because the surfaces of the specimens were dyed, propagation of the pre-imposed tear was detected as nondyed surfaces became exposed.

2.4 Data and Statistical Analysis. Percent composition for collagen, smooth muscle, and elastin was each averaged for all specimens ($n = 12$) from the single vaginal tract, for each region ($n = 4$ for the cranial region, $n = 4$ for the middle region, or $n = 4$ for the caudal region), and for each cross-sectional direction ($n = 6$ for the longitudinal cross section and $n = 6$ for the circumferential cross section). The data were analyzed in this fashion to provide the overall percent composition of the swine vaginal wall, while also examining potential differences by region and direction.

Normalized hook displacement (NHD), defined as the ratio of the average hook distance in the deformed configuration to the average hook distance in the undeformed configuration in the LD or CD, was calculated to compare the specimens across the NT, LT, and CT groups. More specifically, the distances between pairs of hooks, four pairs per direction, were measured using ImageJ and averaged to compute an average hook distance in the LD and CD for both the undeformed and deformed configurations (Fig. 2). The average distances in the undeformed configuration are reported in Table 1. The measurements of the NHD were performed every 15 s of the recorded video for each test.

The average hook distance in the undeformed configuration was also multiplied by specimen initial thickness to calculate the specimen cross-sectional area in the LD or CD. Nominal normal stresses in the LD and CD were calculated by dividing the axial loads by the corresponding cross-sectional areas. This stress quantity will be referred to simply as "stress" hereafter. Using the DIC method, axial local Lagrangian strains in the LD and CD were calculated over a central square region for every specimen in the NT group. The axial local Lagrangian strains were then averaged, resulting in a single average axial Lagrangian strain in the LD and the CD for every second during the test. This average axial Lagrangian strain will be referred to simply as "strain" along the LD or CD hereafter. Local Lagrangian strain was not calculated for the LT or CT group as the strain data in the smaller regions of tissue around the tear and hooks were highly influenced by the boundary conditions. Average stress–strain data for the NT group and average stress-NHD data for each of the three groups were calculated by averaging the stresses at equal strain or NHD, respectively, from every specimen within each group.

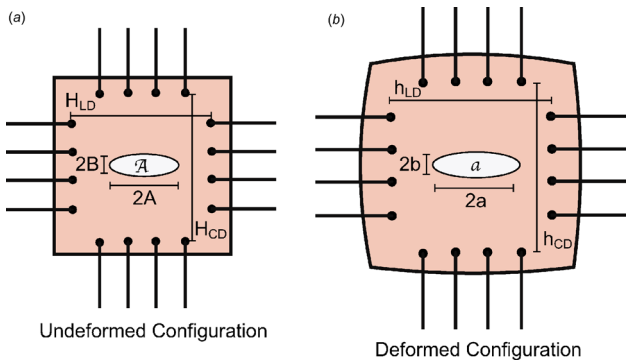

Fig. 2 Schematic of the specimen in the (*a*) undeformed configuration and (*b*) deformed configuration. H_{LD}, H_{CD}, h_{LD}, and h_{CD} represent the distances between hooks in the LD and CD as indicated by the subscripts. 2A and 2a represent the lengths of the major axis of the tear, 2B and 2b represent the lengths of the minor axis of the tear, and $\mathcal{A}$ and a represent the areas of the elliptically shaped tear.

Deformation of the elliptically shaped central tear for the LT and CT groups was determined in ImageJ by measuring the lengths of the major and minor axes and the area of the ellipse at every 15th frame of the recorded video for each test. The area was measured by tracing the boundary of the tear, the lengths of the major and minor axes were measured by drawing two lines across the longest and widest points of the outlined tear. The length of the major axis displacement, a, the length of the minor axis displacement, b, and area of the ellipse, a, in the deformed configuration were divided by the corresponding quantities, A, B, and $\mathcal{A}$ in the undeformed configuration reported in Table 1.

All statistical analysis was performed using a statistical software package (SPSS 25.0; IBM Corp, Armonk, NY). First, the percent composition of collagen, smooth muscle, and elastin in each region and cross-sectional direction was compared with one-way ANOVAs, or Welch ANOVAs when the homogeneity of variances was violated. Second, a paired t-test was conducted to compare the stresses of the NT group in the LD and CD at 15% strain as this was the largest strain achieved across all specimens in the group. None of the assumptions for this test were violated. Third, the stresses in the LD and CD for all three groups were compared at the NHD of 1.05, 1.10, and 1.15 with a two-way mixed ANOVA. None of the assumptions for this analysis were violated. Fourth, a/A and b/B in the LD and CD for the LT and CT groups were compared at an NHD of 1.2, the largest NHD achieved for all specimens in the two groups, with a two-way mixed ANOVA. The data for this analysis contained no outliers and were normally distributed, but the homogeneity of variances ($p < 0.0005$) and homogeneity of covariances ($p < 0.0005$) were violated. The ANOVA revealed a significant interaction between the factors, so simple main effects were examined via Welch ANOVAs and one-way repeated measures ANOVAs with a Greenhouse-Geisser correction when appropriate. Last, a paired t-test was conducted to compare a/A between LT and CT groups at an average NHD of 1.2. None of the assumptions for this test were violated. Statistical significance was set to $p < 0.05$.

3 Results

The average percent composition of smooth muscle, collagen, and elastin across the specimens analyzed from histology is provided in Fig. 3. The swine vaginal wall was found to consist of 31.3 ± 4.9% smooth muscle, 58.9 ± 5.6% collagen, and 1.1 ± 1.5% elastin. No significant differences in percent composition were observed among the cranial, middle, and caudal regions for smooth muscle ($p = 0.05$), collagen ($p = 0.449$), or elastin ($p = 0.155$). There were also no observed significant differences in percent composition between cross sections in the LD and CD for smooth muscle ($p = 0.888$), collagen ($p = 0.331$), or elastin ($p = 0.458$).

Stress–strain curves for the NT group are presented in Fig. 4. All curves were nonlinear and displayed the characteristic toe region of soft tissues. The magnitude of stress or strain up until the specimen was compromised at the hooks was quite variable.

Stresses ranged from 90 to 270 kPa and strains ranged from 15% to 55%. The responses in the LD spanned the entire range of stresses while the responses in the CD spanned the entire range of strains. Comparing the LD to the CD, six specimens appeared stiffer in the LD and three appeared stiffer in the CD. The stiffest response of a specimen occurred in the LD while the most compliant response of a specimen occurred in the CD.

The average stress–strain curves in the LD and CD for the NT group up to 15% strain are presented in Fig. 5. The curves were somewhat nonlinear with very similar behavior up to 10% strain. At higher strains, the curves started to diverge such that the stress at 15% strain was larger in the LD (90 ± 38 kPa) compared to the CD (74 ± 30 kPa), but this was not a statistically significant difference ($p = 0.273$).

Maps of the axial Lagrangian strain in the LD and CD for a representative specimen in the NT group at four time points during testing are reported in Fig. 6. The average strain was larger in the LD than the CD at each time point after the start of the test, but the largest magnitude of strain was only approximately 30% in the LD while approximately 45% in the CD. For the LD, strain increased everywhere within the analyzed region of interest. The strain map in the CD, however, showed horizontal band-like regions across the central portion of the specimen that became more pronounced with the progression of the test. These band-like regions defined alternating regions of high and low strains. Six of the tested specimens displayed this behavior. Interestingly, all six specimens had one or more bands of nearly zero or negative strain in the CD for the duration of the test. Figure 6 displayed strains in the CD of nearly −10% and 45% simultaneously at the last time point within the analyzed region of interest for this specimen.

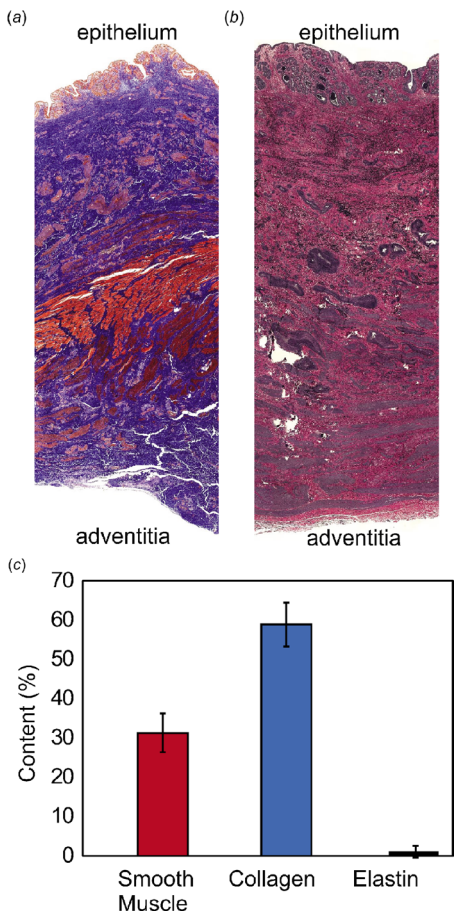

Fig. 3 Histology of full thickness vaginal cross section: (*a*) MT-stained slide and (*b*) VVG-stained slide. (*c*) Percent content of smooth muscle, collagen, and elastin reported as mean ± standard deviation ($n = 12$).

Stress versus NHD curves for the LT and CT groups are shown below in Figs. 7 and 8, respectively. Similar to the NT stress–strain curves, these curves were nonlinear with the characteristic toe region at low NHDs. Stresses and NHDs at hook failure ranged from 100 to 300 kPa and 1.18 to 1.3, respectively, for the LT group and from 100 to 310 kPa and 1.19 to 1.26, respectively, for the CT group. In the LT group, six specimens appeared stiffer in the LD and one specimen appeared stiffer in the CD. In the CT group, four specimens appeared stiffer in the LD and one specimen appeared stiffer in the CD.

The average stress versus NHD for the NT, LT, and CT groups was compared (Fig. 9). No statistically significant differences were observed for NHDs of 1.05 ($p = 0.443$), 1.10 ($p = 0.924$), and 1.15 ($p = 0.513$). There were also no statistically significant differences in stress between directions for the CT group or the LT group at NHDs of 1.05 ($p = 0.274$ and $p = 0.927$, respectively), 1.1 ($p = 0.817$ and $p = 0.368$, respectively), or 1.15 ($p = 0.485$ and $p = 0.135$, respectively). However, there were statistically significant differences in stress between directions for the NT group such that stress in the LD was significantly larger than in the CD at NHDs of 1.05 (16 ± 8 kPa versus 12 ± 4 kPa, $p = 0.049$), 1.10 (45 ± 19 kPa versus 32 ± 8 kPa, $p = 0.045$), and 1.15 (90 ± 39 kPa versus 61 ± 14 kPa, $p = 0.041$). Table 2 summarizes the data presented in Figs. 7–9. Additionally, the average strain was compared to the NHD for the NT group in the LD and CD at NHD values of 1.05, 1.10, and 1.15. This comparison is presented in Table 3.

As the specimen was equibiaxially stretched, the major and minor axes of the elliptically shaped tear were deformed. The

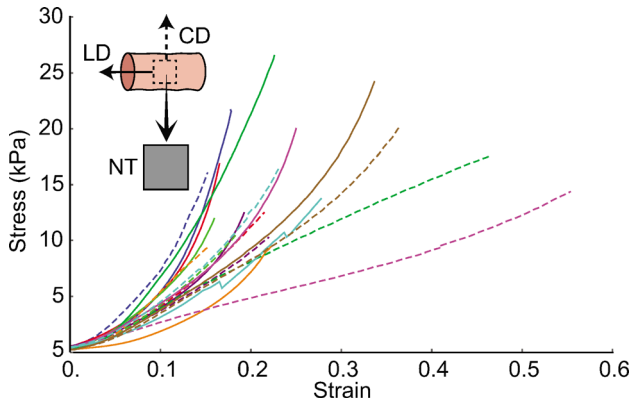

Fig. 4 Stress–strain data in the LD (solid lines) and CD (dashed lines) for specimens in the NT group ($n = 9$)

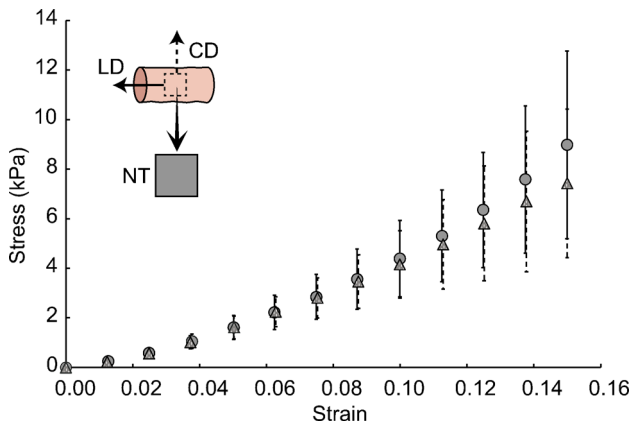

Fig. 5 Mean (± standard deviation) stress–strain data in the LD (solid lines and circles) and CD (dashed lines and triangles) for specimens in the NT group ($n = 9$)

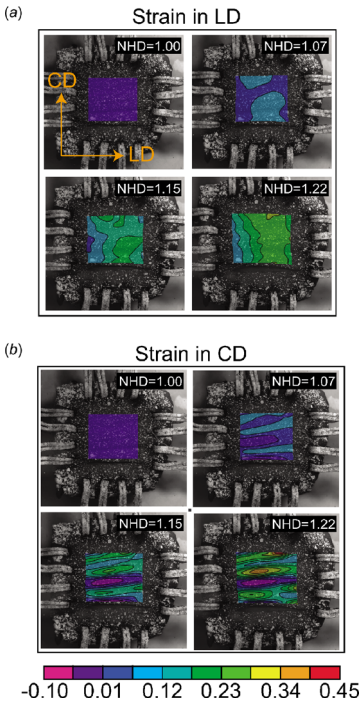

Fig. 6 Axial Lagrangian strain maps in the (*a*) LD and (*b*) CD of a single specimen at four values of NHD

extent of the deformation relative to the NHD for the LT and CT groups is reported in Fig. 10. As shown in Fig. 10(*a*), for the LT group, there was a fairly consistent trend between a/A and NHD, with a/A increasing as NHD increased. However, the relationship between b/B and NHD varied greatly. It was interesting that, for some specimens, b/B increased then decreased with NHD, or, in one case, decreased for the duration of the test. The averages for a/A and NHD in the LD and b/B and NHD in the CD were calculated. Average values of a/A had similar magnitudes to average values of b/B as the average NHD increased such that there was no statistically significant difference in the average a/A and b/B at an average NHD of 1.2 (1.21 ± 0.05 versus 1.18 ± 0.22, $p = 0.756$). As shown in Fig. 10(*b*), for the CT group, there was a linearly increasing trend between a/A and NHD as well as b/B and NHD, but the slope of b/B versus NHD was generally greater than the slope of a/A versus NHD. The variability of b/B was also noticeably less for the CT group compared to the LT group. Averages were again calculated for a/A and NHD in the LD and b/B and NHD in the CD. As the average NHD increased, the average values of b/B became increasingly larger relative to the

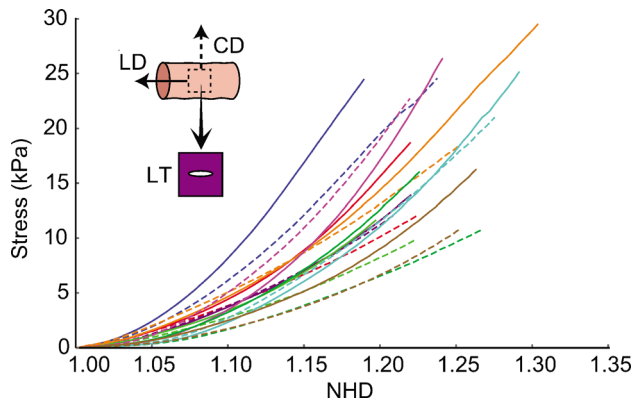

Fig. 7 Stress versus NHD data in the LD (solid lines) and CD (dashed lines) of specimens in the LT group ($n = 9$)

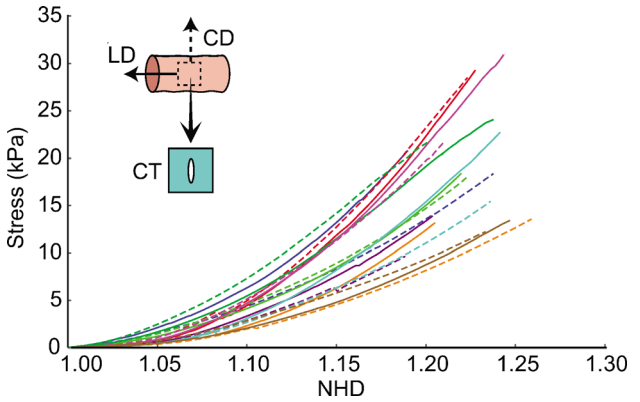

Fig. 8 Stress versus NHD data in the LD (solid lines) and CD (dashed lines) of specimens in the CT group ($n = 9$)

average values of a/A such that b/B was statistically significantly larger than a/A at an average NHD of 1.2 (1.64 ± 0.20 versus 1.21 ± 0.08, $p < 0.0005$). Comparing the average values of a/A and b/B between the LT and CT groups, we found a statistically significant difference in the average values of b/B ($p < 0.0005$) but no statistically significant difference in the average values of a/A ($p = 0.761$) at average NHD values of 1.2.

The normalized changes in areas, $a/\mathcal{A}$, of the tears for the LT and CT groups relative to NHD values that were averaged between the NHD values in the LD and CD were also compared (Fig. 11). The change in areas of the two groups was similar at NHD values up to 1.07 but quickly diverged thereafter. For the CT group, $a/\mathcal{A}$ increased with NHD, but for the LT group, this was not always the case. Averages for $a/\mathcal{A}$ in the two groups as well as total average values for NHD were calculated and compared. At an average NHD of 1.2, the average value of $a/\mathcal{A}$ for the CT group was statistically significantly larger than that of $a/\mathcal{A}$ for the LT group (2.01 ± 0.42 versus 1.40 ± 0.21, $p = 0.003$). Table 4 summarizes the data presented in Figs. 10 and 11.

4 Discussion

In this study, we characterized the mechanical behavior of the swine vaginal tissues under planar equibiaxial tension providing the first analysis of the effect of a pre-imposed elliptically shaped tear on such behavior. Preliminary histological analysis

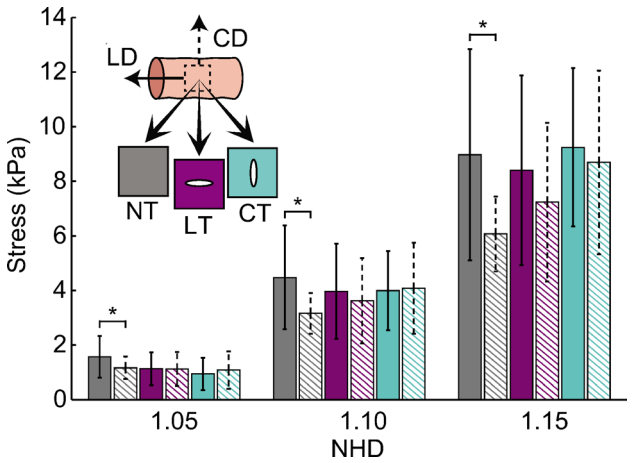

Fig. 9 Mean (± standard deviation) stress data in the LD (solid colored bars with solid lines) and CD (patterned color bars with dashed lines) of the NT ($n = 9$), LT ($n = 9$), and CT ($n = 9$) groups at three levels of NHD. Significant differences in stress were found between the LD and CD for the NT group at all three levels of NHD.

Table 2 Stress versus NHD data for the NT, CT, and LT groups. Average data reported as mean ± standard deviation. Data in bold case represent significant differences between the LD and CD groups, and data ranges reflect the data collected prior to the hooks or central tear compromising the tissue.

	NT		LT		CT	
	LD	CD	LD	CD	LD	CD
Average stress (kPa) NHD = 1.05	**16 ± 8**	**12 ± 4**	11 ± 6	11 ± 6	9 ± 6	11 ± 7
Average stress (kPa) NHD = 1.10	**45 ± 19**	**32 ± 8**	40 ± 18	36 ± 16	40 ± 14	41 ± 17
Average stress (kPa) NHD = 1.15	**90 ± 39**	**61 ± 14**	84 ± 35	72 ± 29	92 ± 29	87 ± 34
Range of stresses (kPa)	90–270	90–200	120–300	100–250	130–310	100–280
Range of NHD	1.16–1.37	1.20–1.38	1.18–1.30	1.21–1.28	1.19–1.25	1.19–1.26

demonstrated some similarities in composition between swine and human vaginas, including the four layer structure [25]. Stress–strain data and remote stress-NHD data displayed a highly nonlinear behavior of the tissue despite the large degree of variability. Stresses in the LD for NHDs up to 1.15 for the NT group were found to be significantly larger than stresses in the CD suggesting some anisotropy of the tissue. Comparing stresses at three NHD values across the NT, LT, and CT groups, no significant differences were found. At NHD values of 1.05, 1.10, and 1.15, a propagation of the central tear for the specimens in the LT and CT groups was not observed, showing the tolerance of the vaginal wall to tears at these levels of NHD. The changes in the tear size strongly depend on the orientation of the major and minor axes of the tear within the vagina. On average, at the NHD value of 1.2, the increases in tear size measured by a/A and b/B were not significantly different for the LT group but significantly different for the CT group where b/B was significantly larger than a/A. Comparing the LT group to the CT group at the NHD value of 1.2, the increase in tear area quantified by $a/\mathcal{A}$ was significantly larger for CT. Collectively, these findings shed some light on the tear tolerance and orientation dependencies of vaginal tissue.

Table 3 Percent difference between average strain and NHD for the NT group in both the LD and CD at NHD values of 1.05, 1.10, and 1.15

NHD	Difference in LD (%)	Difference in CD (%)
1.05	0.36	0.98
1.10	0.47	1.1
1.15	0.8	1.5

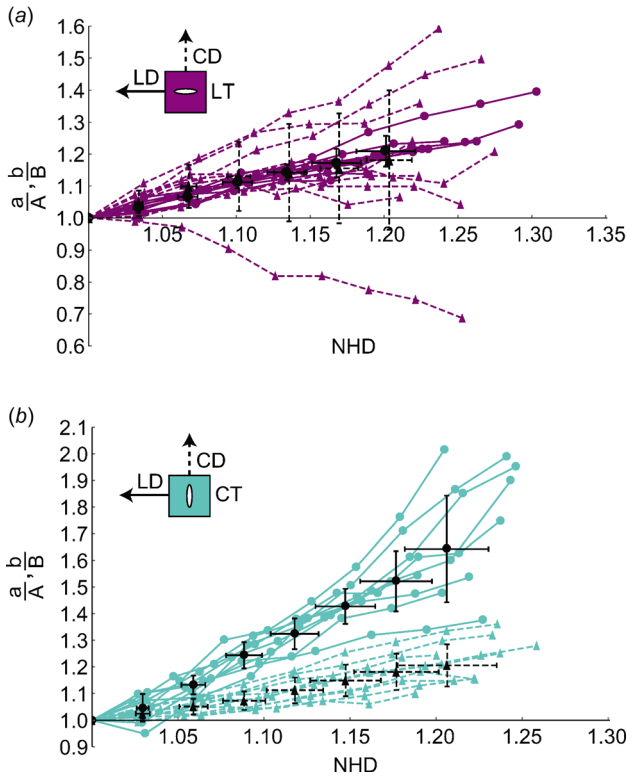

Fig. 10 (*a*) Normalized length, a/A, versus NHD data in the LD (solid lines and circles) and normalized length, b/B, versus NHD data in the CD (dashed lines and triangles) for the LT group ($n = 9$). (*b*) Normalized length, a/A, versus NHD data in the CD (dashed lines and triangles) and normalized length, b/B, versus NHD data in the LD (solid lines and circles) for the CT group ($n = 9$). Mean (±standard deviation) data are also reported (black symbols).

The highly nonlinear stress–strain behavior of swine vaginal tissue, consisting of an extended toe region followed by a stiffer linear region, is typical for soft biological tissues (Figs. 4 and 5). The stress and strain values are within the range of values reported in the literature for different animal models and collected using different experimental protocols [28,39,40]. The linear region was not observed for all specimens due to the different stress and strain values achieved before the specimens were compromised at the hooks during testing. This variation may be due to the inherent variability across the swine, and it may also be due to the differences in the anatomical position of the tested specimens within the vaginal wall (e.g., cranial or caudal position), which was not controlled for. Our preliminary histological analysis on the swine vagina suggested that there are no significant regional differences in composition across anatomical regions. However, other studies have reported such differences in composition [23,22] (Fig. 3). Since our specimens were collected from one sow, additional studies are needed to determine possible differences in composition across regions in the swine vagina. Even so, histology does not provide detailed information about the microstructural

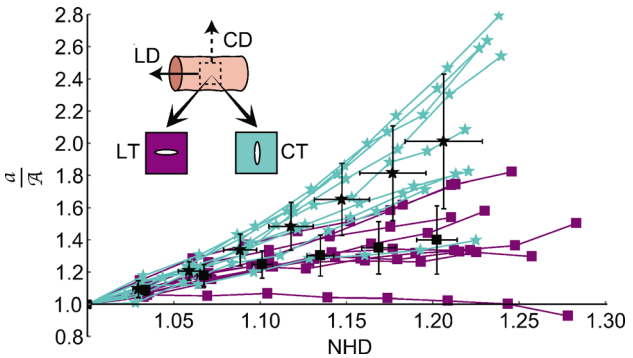

Fig. 11 Normalized changes in the areas, $a/\mathcal{A}$, versus the average of the NHD data in the LD and CD for the LT and CT groups. Mean (± standard deviation) data are also reported (black symbols).

Table 4 Tear deformation versus NHD data for the LT and CT groups. Average data reported as mean±standard deviation. Data in bold case represent significant differences between the LT and CT groups, and data ranges reflect the data collected prior to the hooks or central tear compromising the tissue.

	LT	CT
Average a/A NHD = 1.20	1.21 ± 0.05	1.21 ± 0.08
Average b/B NHD = 1.20	**1.18 ± 0.22**	**1.64 ± 0.20**
Average $a/\mathcal{A}$ NHD = 1.20	**1.40 ± 0.21**	**2.01 ± 0.42**
Range of a/A	1.14–1.40	1.10–1.36
Range of b/B	0.69–1.59	1.37–2.01
Range of $a/\mathcal{A}$	0.93–1.82	1.40–2.80

organization of the tissue's components. Lagrangian strain maps from the specimens in the NT group displayed distinctly different strain behaviors in the LD and CD, which would suggest differences in the organization of the tissue's components along these directions (Fig. 6). It is important to note that the speckle pattern that we tracked for strain measurement was placed on the epithelial layer of the vagina, which is characterized by the presence of rugae. These rugae, usually oriented in the LD, were more easily observable on some specimens than others and likely contributed to the strain behavior in the CD. The lamina propria layer is the major load-bearing layer of the tissue and primarily contains collagen. It extends into the rugae and provides firm contact between the two layers [18]. Therefore, deformation of the epithelial layer very likely reflects the deformation in the underlying lamina propria layer. Quantification of the tissue's microstructural organization would significantly improve our understanding of the complex and variable mechanical behavior of the vaginal tissue. At NHD values of 1.05, 1.10, and 1.15, the stresses of the swine vaginal tissue with pre-imposed tears were not significantly different between the LD and CD (Figs. 7–9). These stresses were not significantly different from the stresses of swine vaginal tissue without a tear (Fig. 9). Of course, while the "remote" stresses in the LT and CT groups were comparable to the stresses in the NT group, the stresses at the tear in the LT and CT groups were likely higher than the stresses in the NT groups due to the stress concentration caused by the presence of the tear. The comparison presented in Fig. 9 may not be particularly useful other than to suggest that the specimens were capable of bearing similar loads in response to the studied deformations regardless of the pre-imposed tears. Others have shown that tears in fibrous tissues, aside from reducing the load-bearing area of the specimens, did not reduce the strength of the specimens, thereby exhibiting high defect tolerances [32].

Several studies have examined the effects of a tear or notch placed in fibrous materials via uniaxial [30,32–34,41] and biaxial tests [34]. It was found in all of these studies that the fibers reorient toward the direction of loading, effectively reinforcing the leading edge of the tear or notch and preventing propagation. The initial tears or notches, rather than propagating through the material like a crack through a brittle material, stretched open and produced a blunting effect. When failure did occur, it was the result of gross material failure rather than the propagation of the initial tear or notch. In soft fibrous tissues, the mobility of water may enable local reinforcement of fibers to a defect [34]. Interestingly, the water content of pregnant tissue increases and may be a protective mechanism of the tissue. We believe the observed toughness of the vaginal tissue at the stretch levels used in this study can be attributed to the reorganization of collagen fibers. However, at larger stretches, the stretching, sliding, and delamination of collagen may provide soft tissues with very high tear resistance [33]. Further mechanical testing coupled with imaging of the microstructure should be carried out to confirm this behavior in vaginal tissues.

The increase in lengths of the major and minor axes of the tear, measured by a/A and b/B, respectively, and the increase in area, measured by $a/\mathcal{A}$, were dependent upon the orientation of the tear within the vaginal tissue (Figs. 10 and 11). For the LT group with specimens having the major axes of the tears oriented in the LD, the averages of a/A and b/B increased similarly at each NHD value. However, for the CT group with specimens having the major axes of the tears oriented in the CD, the average of b/B was significantly larger than the average of a/A. Only the slope of b/B versus NHD for the CT group was larger than 1, indicating a non-affine deformation of the tissue in the vicinity of the tear. Furthermore, the average of $a/\mathcal{A}$ for the CT group was significantly higher from that of the LT group. This clearly indicates that the elliptically shaped tear opened much more when the major axis was oriented in the CD than when oriented in the LD. The swine vaginal tissue appeared to be slightly stiffer in the LD potentially due to the presence of more collagen aligned in this direction. The preferential alignment of fibers in the LD would explain the observed greater resistance to tear propagation in the CD compared with the LD, as well as the larger degree of tear opening observed for the CT group.

The effects of specimen geometry and clamping technique on the mechanical response of soft biological tissues under planar biaxial tests have been studied both experimentally and numerically [42–48]. Mechanical clamps induce stress shielding, with the loads applied through the clamps being redistributed around the edges of the specimen rather than being fully transferred to the central region of the specimen [44,46,48]. This stress-shielding effect has been shown to be more severe for square-shaped specimens compared to cruciform-shaped specimens [46], and it can be mitigated by altering the shape of the cruciform-shaped specimens [47]. On the other hand, when hooks are used for clamping, the loads applied to square-shaped specimens are not uniform and are dependent on hook placement and alignment [45]. By performing some preliminary tests of nitrile rubber and vaginal specimens with pre-imposed tears using hooks with square-shaped specimens and mechanical clamps with cruciform-shaped specimens, we determined that the magnitudes of loads before the specimens failed were comparable. However, cruciform-shaped specimens consistently failed at the arms while square-shaped specimens induced propagation of the central tear. Due to the stress-shielding effect, we preferred to avoid the use of cruciform-shaped specimens for studying the mechanical behavior of the central region of the specimens. Thus, despite the limitations, hooks were chosen to secure square-shaped specimens in order to achieve the largest transfer of loads to the central region of specimens and observe the behavior of the tears.

In this study, an initial tear was imposed on the tissue by cutting a narrow slit with surgical scissors in the center of each specimen. However, upon loading specimens into the biaxial apparatus, it was readily apparent that the imposed cut consistently became elliptical in nature, independently of its initial orientation. Data on the size and shape of perineal and vaginal tears after childbirth are often subjective and dependent on identifiable landmarks [49]. Tools have been developed to measure the sizes of tears, ranging from roughly 20 to 50 mm in the case of second degree tears [50], but the shape of tears is not well documented. The lengths of the tears in this study were kept at the lower end of this range based on the size of the specimens, but the shape of the tears was the result of the tissue behavior. Tears may occur as single tears, as tested in this study, but more complex tearing is known to occur such as branched tears and multiple tear sites. Future work should investigate the formation and shape of tears, the size of tears, and the behavior of more complex tearing as it relates to the mechanical response of vaginal tissue.

Quantifying the stresses and strains that are required to propagate tears within the vaginal wall and characterizing the orientation-dependent behavior of vaginal tears will have profound implications on women's health. Tears that are confined to the vaginal wall usually heal on their own when untreated but, in some cases, they propagate through the layers of the vaginal wall reaching the pelvic muscles, the perineum, and the anal sphincter.

These tears must be treated, and they include second degree perineal tears, which occur at a rate of roughly 25%, third- and fourth-degree perineal tears, which occur at a rate of roughly 5–15%, and nonperineal vaginal tears, which occur at a rate of roughly 20% [7,9,51,52]. Furthermore, third- and fourth-degree perineal tears, as well as nonperineal vaginal tears, are potential markers for levator ani avulsion and can cause anal sphincter injuries, both of which ultimately lead to pelvic floor disorders [12,13,52]. By understanding the mechanisms of tear propagation, new techniques can be developed to prevent severe trauma and protect the perineum and anal sphincter. Toward this end, future work should seek to determine the structure–function relationship of vaginal tissue, especially as it changes through pregnancy when tears are more likely to occur.

5 Conclusions

The deformations and tear behavior of the swine vaginal tissue were studied in response to planar equibiaxial tension. The tissue was highly nonlinear and somewhat anisotropic being, on average, stiffer in the LD than in the CD. When comparing the remote stresses of specimens without a tear and with pre-imposed elliptically shaped tears with major axes aligned in the LD and CD, no significant differences were found for NHD up to 1.15. This indicates that the remote stresses of the vaginal wall are unaltered by the presence of tears and their orientation. Furthermore, no tears were observed to propagate for NHDs less than 1.15, but elliptically shaped tears with their major axes aligned to the CD deformed significantly more than tears with their major axes aligned to the LD. The tissue microstructure likely confers the high tear resistance to the vaginal tissue and dictates the orientation dependent behavior of the tear. Knowledge about the role of the tissue microstructure on the complex mechanical behavior of the vagina will serve to select appropriate methods for preventing tears and mitigating the risk of severe complications.

Acknowledgment

The authors would like to thank Dr. Adwoa Baah-Dwomoh for her assistance with tissue collection and histology, Duncan Stebelton for his assistance with analysis of histology, and Dr. Marianna Alperin, University of California, San Diego, for very insightful discussions.

Funding Data

- Division of Chemical, Bioengineering, Environmental, and Transport Systems (1511603, Funder ID. 10.13039/100000146).
- National Science Foundation NSF (Grant No. 1511603, Funder ID. 10.13039/100000001).

References

[1] Ramin, S., Satin, A., Stone, J. I., and Wendel, J. G., 1992, "Sexual Assault in Postmenopausal Women," Obstet. Gynecol., **80**(5), pp. 860–864.
[2] Sau, A., Dhar, K., and Dhall, G., 1993, "Nonobstetric Lower Genital Tract Trauma," Aust. N. Z. J. Obstet. Gynaecol., **33**(4), pp. 433–435.
[3] McLean, I., Roberts, S., White, C., and Paul, S., 2011, "Female Genital Injuries Resulting From Consensual and Non-Consensual Vaginal Intercourse," Forensic Sci. Int., **204**(1–3), pp. 27–33.
[4] Campbell, S., and Newman, G., 1971, "Growth of the Fetal Biparietal Diameter During Normal Pregnancy," BJOG: An Int. J. Obstet. Gynaecol., **78**(6), pp. 513–519.
[5] Barnhart, K., Izquierdo, A., Pretorius, E., Shera, D., Shabbout, M., and Shaunik, A., 2006, "Baseline Dimensions of the Human Vagina," Hum. Reprod., **21**(6), pp. 1618–1622.
[6] Samuelsson, E., Ladfors, L., Lindblom, B., and Hagberg, H., 2002, "A Prospective Observational Study on Tears During Vaginal Delivery: Occurrences and Risk Factors," Acta Obstet. Gynecol. Scand., **81**(1), pp. 44–49.
[7] Hopkins, L., Caughey, A., Glidden, D., and Laros, R., 2005, "Racial/Ethnic Differences in Perineal, Vaginal and Cervical Lacerations," Am. J. Obstet. Gynecol., **193**(2), pp. 455–459.
[8] Andrews, V., Sultan, A., Thakar, R., and Jones, P., 2006, "Occult Anal Sphincter Injuries—Myth or Reality?," BJOG: An Int. J. Obstet. Gynaecol., **113**(2), pp. 195–200.
[9] Gurol-Urganci, I., Cromwell, D., Edozien, L., Mahmood, T. A., Adams, E., Richmond, D., Templeton, A., and Meulen, J., 2013, "Third-and Fourth-Degree Perineal Tears Among Primiparous Women in England Between 2000 and 2012: Time Trends and Risk Factors," BJOG: An Int. J. Obstet. Gynaecol., **120**(12), pp. 1516–1525.
[10] Martin, J., Hamilton, B., Osterman, M., Driscoll, A., and Matthews, T., 2017, "Births: Final Data for 2015," Natl. Vital Stat. Rep., **66**(1), pp. 1–70.
[11] Riesner, M., and Polley, L., 2007, "Chapter 194—Postpartum Hemorrhage," *Complications in Anesthesia*, 2nd ed., J. Atlee, ed., W. Saunders, Philadelphia, PA, pp. 779–781.
[12] Sultan, A., Kamm, M., Hudson, C., Thomas, J., and Bartram, C., 1993, "Anal-Sphincter Disruption During Vaginal Delivery," New Engl. J. Med., **329**(26), pp. 1905–1911.
[13] Borello-France, D., Burgio, K. L., Richter, H. E., Zyczynski, H., FitzGerald, M. P., Whitehead, W., Fine, P., Nygaard, I., Handa, V. L., Visco, A. G., and Weber, A. M., 2006, "Fecal and Urinary Incontinence in Primiparous Women," Obstet. Gynecol., **108**(4), pp. 863–872.
[14] Macarthur, A., and Macarthur, C., 2004, "Incidence, Severity, and Determinants of Perineal Pain After Vaginal Delivery: A Prospective Cohort Study," Am. J. Obstet. Gynecol., **191**(4), pp. 1199–1204.
[15] Williams, A., Lavender, T., Richmond, D., and Tincello, D., 2005, "Women's Experiences After a Third-Degree Obstetric Anal Sphincter Tear: A Qualitative Study," Birth, **32**(2), pp. 129–136.
[16] Williams, A., Herron-Marx, S., and Carolyn, H., 2007, "The Prevalence of Enduring Postnatal Perineal Morbidity and Its Relationship to Perineal Trauma," Midwifery, **23**(4), pp. 392–403.
[17] Fernando, R., and Sultan, A., 2004, "Risk Factors and Management of Obstetric Perineal Injury," Obstet., Gynaecol. Reprod. Med., **14**(5), pp. 320–326.
[18] Krstic, R., 2013, *Human Microscopic Anatomy: An Atlas for Students of Medicine and Biology*, Springer , Berlin.
[19] Boreham, M., Wai, C., Miller, R., Schaffer, J., and Word, R., 2002, "Morphometric Analysis of Smooth Muscle in the Anterior Vaginal Wall of Women With Pelvic Organ Prolapse," Am. J. Obstet. Gynecol., **187**(1), pp. 56–63.
[20] Takano, C. C., Gira, M. J., Sartori, M. G., Castro, R. A., Arruda, R. M., Simo, M. J., Baracat, E. C., and de Lima, G. R., 2002, "Analysis of Collagen in Parametrium and Vaginal Apex of Women With and Without Uterine Prolapse," Int. Urogynecol. J., **13**(6), pp. 342–345.
[21] Ulrich, D., Edwards, S., Su, K., White, J., Ramshaw, J., Jenkin, G., Deprest, J., Rosamilia, A., Werkmeister, J., and Gargett, C., 2014, "Influence of Reproductive Status on Tissue Composition and Biomechanical Properties of Ovine Vagina," PLoS One, **9**(4), p. e93172.
[22] Ulrich, D., Edwards, S., Letouzey, V., Su, K., White, J., Rosamilia, A., Gargett, C., and Werkmeister, J., 2014, "Regional Variation in Tissue Composition and Biomechanical Properties of Postmenopausal Ovine and Human Vagina," PLoS One, **9**(8), p. e104972.
[23] Rynkevic, R., Martins, P., Hympanova, L., Almeida, H., Fernandes, A., and Deprest, J., 2017, "Biomechanical and Morphological Properties of the Multiparous Ovine Vagina and Effect of Subsequent Pregnancy," J. Mech., **57**, pp. 94–102.
[24] Badiou, W., Granier, G., Bousquet, P., Monrozies, X., Mares, P., and de Tayrac, R., 2008, "Comparative Histological Analysis of Anterior Vaginal Wall in Women With Pelvic Organ Prolapse or Control Subjects—A Pilot Study," Int. Urogynecol. J., **19**(5), pp. 723–729.
[25] Kerkhof, M., Ruiz-Zapata, A., Bril, H., Bleeker, M., Belien, J., Stoop, R., and Helder, M., 2014, "Changes in Tissue Composition of the Vaginal Wall of Premenopausal Women With Prolapse," Am. J. Obstet. Gynecol., **210**(2), p. 168.
[26] Sridharan, I., Ma, Y., Kim, T., Kobak, W., Rotmensch, J., and Wang, R., 2012, "Structural and Mechanical Profiles of Native Collagen Fibers in Vaginal Wall Connective Tissues," Biomaterials, **33**(5), pp. 1520–1527.
[27] Baah-Dwomoh, A., McGuire, J., Tan, T., and De Vita, R., 2016, "Mechanical Properties of Female Reproductive Organs and Supporting Connective Tissues: A Review of the Current State of Knowledge," ASME Appl. Mech. Rev., **68**(6), p. 060801.
[28] Robison, K., Conway, C., Desrosiers, L., Knoepp, L., and Miller, K., 2017, "Biaxial Mechanical Assessment of the Murine Vaginal Wall Using Extension–Inflation Testing," ASME J. Biomech. Eng., **139**(10), p. 104504.
[29] Oyen-Tiesma, M., and Cook, R., 2001, "Technique for Estimating Fracture Resistance of Cultured Neocartilage," J. Mater. Sci.: Mater. Med., **12**(4), pp. 327–332.
[30] Stok, K., and Oloyede, A., 2003, "A Qualitative Analysis of Crack Propagation in Articular Cartilage at Varying Rates of Tensile Loading," Connect. Tissue Res., **44**(2), pp. 109–120.
[31] Fessel, G., Wernli, J., Li, Y., Gerber, C., and Snedeker, J., 2012, "Exogenous Collagen Cross-Linking Recovers Tendon Functional Integrity in an Experimental Model of Partial Tear," J. Orthop. Res., **30**(6), pp. 973–981.
[32] Taylor, D., O'Mara, N., Ryan, E., Takaza, M., and Simms, C., 2012, "The Fracture Toughness of Soft Tissues," J. Mech. Behav. Biomed. Mater., **6**, pp. 139–147.
[33] Yang, W., Sherman, V., Gludovatz, B., Schaible, E., Stewart, P., Ritchie, R., and Meyers, M., 2015, "On the Tear Resistance of Skin," Nat. Commun., **6**, p. 6649.
[34] Ehret, A., Bircher, K., Stracuzzi, A., Marina, V., Zündel, M., and Mazza, E., 2017, "Inverse Poroelasticity as a Fundamental Mechanism in Biomechanics and Mechanobiology," Nat. Commun., **8**(1), p. 1002.
[35] Bal, H., and Getty, R., 1972, "Vaginal Histology of the Domestic Pig: Histomorphology From Birth to 8 Years With Some Clinical Aspects," J. Reprod. Fertil., **28**(1), pp. 1–7.

[36] Gruber, D., Warner, W., Lombardini, E., Zahn, C., and Buller, J., 2011, "Anatomical and Histological Examination of the Porcine Vagina and Supportive Structures: In Search of an Ideal Model for Pelvic Floor Disorder Evaluation and Management," Female Pelvic Med. Reconstr. Surg., **17**(3), pp. 110–114.
[37] Sutton, M., Orteu, J., and Schreier, H., 2009, *Image Correlation for Shape, Motion and Deformation Measurements*, Springer, New York.
[38] Lionello, G., Sirieix, C., and Baleani, M., 2014, "An Effective Procedure to Create a Speckle Pattern on Biological Soft Tissue for Digital Image Correlation Measurements," J. Mech. Behav. Biomed. Mater., **39**, pp. 1–8.
[39] Rubod, C., Boukerrou, M., Brieu, M., Dubois, P., and Cosson, M., 2007, "Biomechanical Properties of Vaginal Tissue—Part 1: New Experimental Protocol," J. Urol., **178**(1), pp. 320–325.
[40] Rubod, C., Boukerrou, M., Brieu, M., Jean-Charles, C., Dubois, P., and Cosson, M., 2008, "Biomechanical Properties of Vaginal Tissue: Preliminary Results," Int. Urogynecol. J., **19**(6), pp. 811–816.
[41] Koh, C., Strange, D., Tonsomboon, K., and Oyen, M., 2013, "Failure Mechanisms in Fibrous Scaffolds," Acta Biomater., **9**(7), pp. 7326–7334.
[42] Waldman, S., and Lee, J., 2002, "Boundary Conditions During Biaxial Testing of Planar Connective Tissues—Part 1: Dynamic Behavior," J. Mater. Sci.: Mater. Med., **13**(10), pp. 933–938.
[43] Waldman, S., Sacks, M., and Lee, J., 2002, "Boundary Conditions During Biaxial Testing of Planar Connective Tissues—Part II: Fiber Orientation," J. Mater. Sci. Lett., **21**(15), pp. 1215–1221.
[44] Sun, W., Sacks, M., and Scott, M., 2005, "Effects of Boundary Conditions on the Estimation of the Planar Biaxial Mechanical Properties of Soft Tissues," ASME J. Biomech. Eng., **127**(4), pp. 709–715.
[45] Eilaghi, A., Flanagan, J., Brodland, G., and Ethier, C., 2009, "Strain Uniformity in Biaxial Specimens Is Highly Sensitive to Attachment Details," ASME J. Biomech. Eng., **131**(9), p. 091003.
[46] Jacobs, N., Cortes, D., Vresilovic, E., and Elliott, D., 2013, "Biaxial Tension of Fibrous Tissue: Using Finite Element Methods to Address Experimental Challenges Arising From Boundary Conditions and Anisotropy," ASME J. Biomech. Eng., **135**(2), p. 021004.
[47] Zhao, X., Berwick, Z., Krieger, J., Chen, H., Chambers, S., and Kassab, G., 2014, "Novel Design of Cruciform Specimens for Planar Biaxial Testing of Soft Materials," Exp. Mech., **54**(3), pp. 343–356.
[48] Nolan, D., and McGarry, J., 2016, "On the Correct Interpretation of Measured Force and Calculation of Material Stress in Biaxial Tests," J. Mech. Behav. Biomed. Mater., **53**, pp. 187–199.
[49] Cioffi, J., Swain, J., and Arundell, F., 2010, "The Decision to Suture After Childbirth: Cues, Related Factors, Knowledge and Experience Used by Midwives," Midwifery, **26**(2), pp. 246–255.
[50] Metcalfe, A., Tohill, S., Williams, A., Haldon, V., Brown, L., and Henry, L., 2002, "A Pragmatic Tool for the Measurement of Perineal Tears," B. J. Midwifery, **10**(7), pp. 412–417.
[51] Edozien, L., Gurol-Urganci, I., Cromwell, D., Adams, E., Richmond, D., Mahmood, T., and Meulen, J., 2014, "Impact of Third-and Fourth-degree Perineal Tears at First Birth on Subsequent Pregnancy Outcomes: A Cohort Study," BJOG: An Int. J. Obstet. Gynaecol., **121**(13), pp. 1695–1703.
[52] Shek, K., Green, K., Hall, J., Guzman-Rojas, R., and Dietz, H., 2016, "Perineal and Vaginal Tears Are Clinical Markers for Occult Levator Ani Trauma: A Retrospective Observational Study," Ultrasound Obstet. Gynecol., **47**(2), pp. 224–227.